Precision Synthesis of a Fluorinated Polyhedral Oligomeric Silsesquioxane-Terminated Polymer and Surface Characterization of Its Blend Film with Poly(methyl methacrylate)

Kyoungmoo Koh,[†] Satoshi Sugiyama,[†] Takashi Morinaga,[†] Kohji Ohno,[†] Yoshinobu Tsujii,[†] Takeshi Fukuda,*[,†] Mikio Yamahiro,[‡] Takashi Iijima,[‡] Hisao Oikawa,[‡] Kenichi Watanabe,[‡] and Tokuji Miyashita[§]

Institute for Chemical Research, Kyoto University, Uji, Kyoto 611-0011, Japan; Goi Research Center, Chisso Petrochemical Corporation, 5-1 Goi-Kaigan, Ichihara, Chiba 290-8551, Japan; and Institute for Multidisciplinary Research for Advanced Materials, Tohoku University, 2-1-1 Katahira, Aoba-ku, Sendai 980-8577, Japan

Received November 17, 2004; Revised Manuscript Received December 9, 2004

ABSTRACT: Incompletely condensed, fluorinated polyhedral oligomeric silsesquioxane with the highly reactive group of trisodium silanolate was used for the synthesis of an initiator for atom transfer radical polymerization. The initiator was applied to solution polymerization of methyl methacrylate (MMA) in the presence of a copper complex. The polymerization proceeded in a living fashion, providing tadpole-shaped polymers with an "inorganic head" of polyhedral oligomeric silsesquioxane (POSS) and an "organic tail" of well-defined PMMA. A blend film composed of the tadpole-shaped polymer and a matrix PMMA was annealed at 180 °C for 5 days and then analyzed by neutron reflectometry, X-ray photoelectron spectroscopy, and contact angle measurement. These analyses revealed that the tadpole-shaped polymer was preferentially populated at the air/polymer interface, and the outermost layer of the film was almost completely covered by the POSS heads. This was mainly due to the low surface free energy of the fluorinated POSS moiety. Owing to this unique structure, the blend film showed strong resistance against Ar^+ ion etching, despite the overall POSS content was only 2 wt %.

Introduction

Polyhedral oligomeric silsesquioxane (POSS) is a cube-octameric molecule with an inner inorganic Si−O−Si framework that is externally covered by organic substituents.[1] Thanks to the establishment of reliable methods for the synthesis of a number of POSS-based chemicals that contain various combinations of nonreactive substituents and/or reactive functionalities, POSS moieties can be incorporated into polymer systems via polymerization, grafting, blending, and so forth.[2−13] Such hybridizations result in dramatic improvement of polymer properties including glass transition and degradation temperatures, flammability, mechanical strength, and oxygen permeability.[14−18]

The surface (or air/polymer interface) structures of multicomponent polymer systems such as block and random copolymers and polymer blends are usually different from those of the bulk, depending on monomer and polymer compositions, chain architecture, and chain-end functionalities.[19,20] Such phenomena are strongly emphasized by the use of fluorinated materials: for example, their low surface free energies will drive themselves toward the surface.[21−25]

In this study, we focus on the improvement of the surface properties of a polymeric thin film by utilizing the inherent characters of POSS and fluorine atom. We recently developed a technique for the synthesis of fluorinated POSS derivatives from an incompletely condensed POSS with the highly reactive group of trisodium silanolate[26] and also one for the synthesis of a tadpole-shaped hybrid polymer with an "inorganic head" of POSS and an "organic tail" of well-defined polymer[27] by atom transfer radical polymerization[28] (ATRP). Combining these two techniques, we here prepare a new tadpole-shaped polymer composed of a fluorinated POSS and a well-defined polymer. The surface and structural characterization of the thin blend film composed of the tadpole-shaped polymer and poly(methyl metacrylate) are carried out by neutron reflectometry, X-ray photoelectron spectroscopy, and contact angle measurement. The surface hardness of the blend film is evaluated by studying its resistance against Ar^+ ion etching.

Experimental Section

Materials. AK-225 (the mixture of $CF_3CF_2CHCl_2$ and $CClF_2CF_2CHClF$) was obtained from Asahi Glass Co., Ltd., Tokyo, Japan, and used without further purification. Ethyl 2-bromoisobutylate (98%, 2-(EiB)Br) was used as received from Nacalai Tesque Inc., Osaka, Japan. Methly methacrylate (99%, MMA) was obtained from Nacalai Tesque Inc. and distilled under reduced pressure over calcium hydride. *N*,*N*′-Dimethylformamide (99.5%, DMF) was purchased from Nacalai Tesque Inc. Copper(I) chloride (99.9%, Cu(I)Cl) was purchased from Wako Pure Chemicals, Osaka, Japan. 4,4′-Dinonyl-2,2′-bipyridine (97%, dNbipy) was purchased from Aldrich and used without further purification. All other reagents were used as received from commercial sources.

Measurements. Gel permeation chromatographic (GPC) analysis was carried out at 40 °C on a Shodex GPC-101 high-speed liquid chromatography system equipped with a guard column (Shodex GPC KF-G), two 30 cm mixed columns (Shodex GPC KF-804L, exclusion limit = 400 000), and a differential refractometer (Shodex RI-101). Tetrahydrofuran (THF) was used as an eluent at a flow rate of 0.8 mL/min. Poly(methyl methacrylate) (PMMA) standards were used to calibrate the GPC system.

[†] Kyoto University.
[‡] Chisso Petrochemical Corp.
[§] Tohoku University.
* To whom correspondence should be addressed: e-mail fukuda@scl.kyoto-u.ac.jp.

10.1021/ma047636l CCC: $30.25
Published on Web 01/28/2005

Scheme 1. Synthesis of Fluorinated POSS-Holding Initiator 7F-T_8-BIB

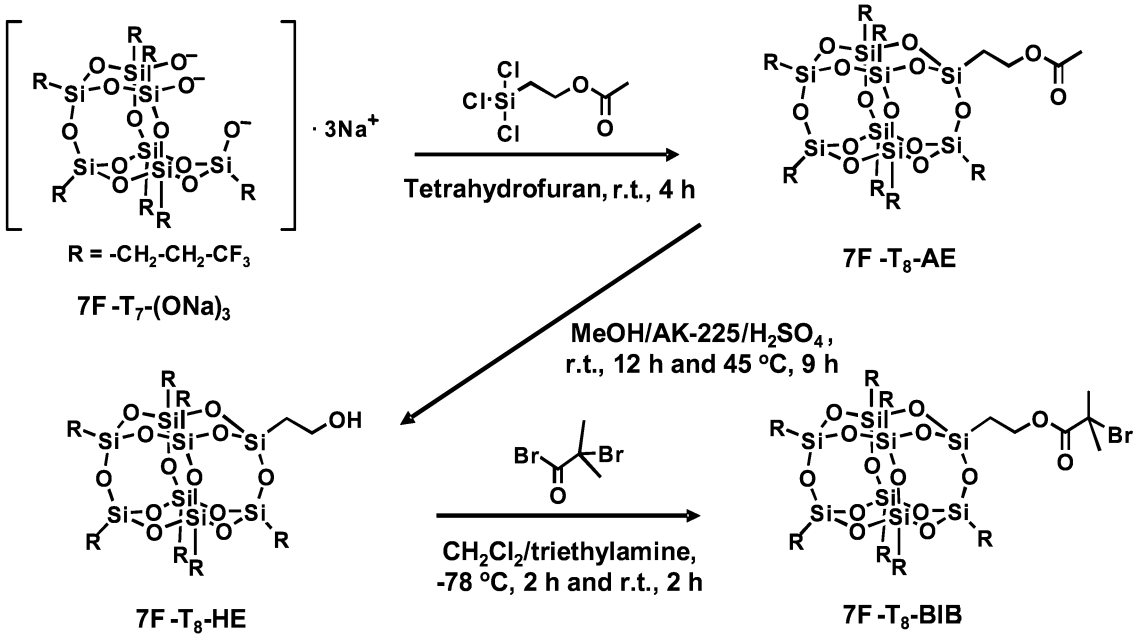

Nuclear magnetic resonance (^{1}H, ^{13}C, and ^{29}Si NMR) spectra were obtained on a JEOL/AL400 400 MHz spectrometer. Deuterated chloroform ($CDCl_3$) was used as a solvent.

Ellipsometric analysis was performed on a variable angle-of-incidence spectroscopic ellipsometer (M-2000U, J. A. Woollam Co., Inc.). Measurements were taken at three incidence angles of 65°, 70°, and 75°. The ellipsometric angles were recorded in a wavelength range from 242 to 999 nm. The data were processed and fitted by the software WVASE32 (J. A. Woollam Co., Inc.).

Neutron reflectometric measurements were performed on a time-of-flight neutron reflectometer (PORE)[29] at the Neutron Science Laboratory, Institute of Materials Structure Science High Energy Accelerator Research Organization, Tsukuba, Japan. The cold neutron beam with wavelengths ranging from 0.3 to 2 nm was incident from the air side of the sample at incident angles θ of 0.25° and 0.6°. The angular resolution $\Delta\theta/\theta$ was 5%. The specular reflection was measured by the time-of-flight method using a ^{3}H proportional counter. The reflectivity R was analyzed on the basis of the multilayered model using spreadsheet environment reflectivity fitting (SERF).[30]

Angle-dependent X-ray photoelectron spectroscopic (XPS) measurements were made on a PHI 5600 spectrometer (Perkin-Elmer Inc.) equipped with a multiple channel detector. The Mg Kα X-ray source (1253.6 eV) was operated at 400 W (14 kV and 28.6 mA). The system pressure was less than 7.0×10^{-9} Torr. High-resolution spectra were acquired over a 20 eV window with a pass energy of 58.7 eV at 0.125 eV/step. Each sample was analyzed at takeoff angles (the angles between the photoelectron emission direction and the sample surface) of 15°, 30°, 45°, 60°, 75°, and 90°. All binding energies were referenced to the C 1s peak for neutral carbon, which was assigned a value of 285.0 eV.

Static contact angle measurements were performed at 20 °C and ambient humidity on a CA-X contact angle meter (Kyowa Interface Science Co., Ltd.) equipped with a video capture apparatus. Water and diiodomethane were used as probe liquids. A liquid drop (1.8 μL) was deposited on a sample surface with a microsyringe. Contact angles were measured at five different positions for one sample and averaged.

Synthesis of 2-Bromoisobutyryloxyethylhepta(3,3,3-trifluoropropyl)-T_8-silsesquioxane (7F-T_8-BIB, Scheme 1). 7F-T_8-BIB was synthesized via the four-step reactions described below. First, (3,3,3-trifluoropropyl)trimethoxysilane (100 g, 0.46 mol), THF (500 mL), distilled water (10.5 g, 0.58 mol), and sodium hydroxide (7.9 g, 0.2 mol) were charged into a four-necked flask equipped with a reflux condenser and a thermometer. The mixture was refluxed in an oil bath thermostated at 70 °C for 5 h with magnetically stirring. The system was allowed to get cool to room temperature and left for 15 h. The volatile components were removed by heating at 95 °C under atmospheric pressure to obtain a white precipitate, which was collected by a membrane filter having a pore diameter of 0.5 μm, washed with THF, and dried at 80 °C for 3 h in a vacuum oven to yield hepta(3,3,3-trifluoropropyl)-tricycloheptasiloxane trisodium silanolate (7F-T_7-$(ONa)_3$, Scheme 1) as a white powder (74 g, 65 mmol) in a quantitative yield. Because of the low solubility of 7F-T_7-$(ONa)_3$, its high purity was confirmed by characterizing the product 7F-T_7-$(OTMS)_3$ obtained by the reaction of 7F-T_7-$(ONa)_3$ with trimethylchlorosilane (see Supporting Information).

Second step: 7F-T_7-$(ONa)_3$ (22.7 g, 19.9 mmol), triethylamine (2 g, 19.9 mol), and dry THF (450 mL) were charged into a round-bottomed flask, to which acetoxyethyltrichlorosilane (7 g, 31.8 mmol) was quickly added at room temperature. The mixture was magnetically stirred for 4 h at room temperature. The resultant precipitate was removed by filtration, and the filtrate was concentrated by a rotary evaporator to obtain a crude product. The resultant solid was dispersed in methanol (MeOH, 100 mL), collected with a membrane filter, and dried at 75 °C for 5 h to yield acetoxyethylheptatrifluoropropyl-T_8-silsesquioxane (7F-T_8-AE) as a white solid (15.5 g, 13.1 mmol, 66%). ^{1}H NMR ($CDCl_3$, 400 MHz): δ 4.18 (t, 2H, $-O-CH_2-$), 2.14 (m, 14H, $-CH_2-CF_3$), 2.04 (s, 3H, $CH_3-C=O$), 1.19 (t, 2H, $-CH_2-Si$), 0.95 (m, 14H, $Si-CH_2-CH_2-CF_3$). ^{13}C NMR ($CDCl_3$, 100 MHz): δ 171.11 ($C=O$), 131.41, 128.68, 125.92, and 123.20 ($-CF_3$), 60.01 ($-O-CH_2-$), 28.17, 27.85, 27.55, and 27.25 ($-CH_2-CF_3$), 20.92 ($CH_3-C=O$), 12.81 ($-CH_2-Si$), 4.03 ($Si-CH_2-CH_2-CF_3$). ^{29}Si NMR ($CDCl_3$, 79 MHz): δ −68.66 ($-CH_2-SiO_{1.5}$), −67.62 and −67.72 ($CF_3-CH_2-CH_2-SiO_{1.5}$).

Third step: 7F-T_8-AE (3.5 g, 2.96 mmol), MeOH (360 mL), and AK-225 (240 mL) were charged in a round-bottomed flask, to which concentrated H_2SO_4 (0.9 mL) was added at room temperature. The mixture was magnetically stirred for 12 h at room temperature and another 9 h at 45 °C and then concentrated by a rotary evaporator. The oily residue was redissolved in AK-225 (200 mL) and washed twice with water (2×500 mL). The organic layer was collected and dried over anhydrous $MgSO_4$. After filtration, the filtrate was concentrated by a rotary evaporator and dried in a vacuum oven to obtain hydroxylethylheptatrifluoropropyl-T_8-silsesquioxane

(7F-T_8-HE) (3 g, 2.62 mmol, 90%). ^{1}H NMR ($CDCl_3$, 400 MHz): δ 3.81 (t, 2H, $-O-CH_2-$), 2.14 (m, 14H, $-CH_2-CF_3$), 1.39 (broad, 1H, $-OH$), 1.13 (t, 2H, $-CH_2-CH_2-Si$), 0.93 (m, 14H, $Si-CH_2-CH_2-CF_3$). ^{13}C NMR ($CDCl_3$, 100 MHz): δ 131.31, 128.58, 125.83, and 123.11 ($-CF_3$), 58.08 ($-CH_2-OH$), 28.12, 27.83, 27.52, and 27.22 ($-CH_2-CF_3$), 19.74 ($-CH_2-Si$), 4.02 ($Si-CH_2-CH_2-CF_3$). ^{29}Si NMR ($CDCl_3$, 79 MHz): δ -67.84 ($-CH_2-SiO_{1.5}$), -67.65 and -67.66 ($CF_3-CH_2-CH_2-SiO_{1.5}$).

Fourth step: 2-bromoisobutyryl bromide (1.2 g, 5.5 mmol) was added to a cold solution of 7F-T_8-HE (2.9 g, 2.5 mmol) in dry dichloromethane (50 mL) with triethylamine (500 mg, 4.9 mmol) at -78 °C. The mixture was magnetically stirred for 1 h at -78 °C and then another 2 h at room temperature. After filtration, the filtrate was diluted with dichloromethane (500 mL) and washed with water (500 mL), twice with 1 wt % of aqueous $NaHCO_3$ solution (2 × 500 mL), and again twice with water (2 × 500 mL). After drying over $MgSO_4$ and filtration, the filtrate was concentrated by a rotary evaporator. Toluene (500 mL) was added into the resultant residue, and the mixture was kept in a freezer to obtain a precipitate, which was washed with MeOH (500 mL), collected by a membrane filter, and dried at 40 °C for 6 h to yield the final product 7F-T_8-BIB as a white solid (2.29 g, 1.75 mmol, 70%). ^{1}H NMR ($CDCl_3$, 400 MHz): δ 4.28 (t, 2H, $-O-CH_2-$), 2.15 (m, 14H, $-CH_2-CF_3$), 1.93 (s, 6H, $-CBr-(CH_3)_2$), 1.25 (t, 2H, $-O-CH_2-CH_2-Si$), 0.94 (m, 14H, $Si-CH_2-CH_2-CF_3$). ^{13}C NMR ($CDCl_3$, 100 MHz): δ 171.23 ($C{=}O$), 131.32, 128.57, 125.79, and 123.07 ($-CF_3$), 61.83 ($-O-CH_2-$), 55.80 ($-CBr$), 30.70 ($(-CH_3)_2$), 28.13, 27.83, 27.52, and 27.23 ($-CH_2-CF_3$), 12.45 ($-O-CH_2-CH_2-Si$), 4.00 ($Si-CH_2-CH_2-CF_3$). ^{29}Si NMR ($CDCl_3$, 79 MHz): δ -69.02 ($-CH_2-SiO_{1.5}$), -67.67 and -67.73 ($CF_3-CH_2-CH_2-SiO_{1.5}$). Anal. Calcd for $C_{27}H_{38}O_{14}F_{21}BrSi_8$: C, 25.14; H, 2.96; F, 30.92; Br, 6.19. Found: C, 24.98; H, 2.97; F, 30.96; Br, 5.74.

ATRP of MMA by 7F-T_8-BIB. A Schlenk tube was charged with DMF (4 mL), MMA (4 g, 40 mmol), 7F-T_8-BIB (130 mg, 0.1 mmol), and dNbipy (82 mg, 0.2 mmol), and then the mixture was deoxygenated by purging with argon for 5 min. To this mixture, Cu(I)Cl (10 mg, 0.1 mmol) was added in a glovebox purged with argon, and the Schlenk tube was equipped with a three-way stopcock. The polymerization was carried out in a shaking oil bath thermostated at 70 °C, and after a prescribed time t, an aliquot of the solution was taken out for NMR measurement to estimate monomer conversion and for GPC measurement. The rest of the sample was diluted by THF and added in an excess of n-hexane to obtain a polymer fPOSS−PMMA as a white powder. To characterize the PMMA chain grown from the POSS initiator, the POSS moiety of the fPOSS−PMMA was decomposed as follows: the fPOSS−PMMA (15 mg) dissolved in toluene (2 mL) was charged into a polyethylene tube, to which a 12 wt % aqueous HF solution (4 mL) and methyltrioctylammonium chloride (20 mg) as a phase transfer catalyst were added. The mixture was vigorously stirred for 12 h. The organic layer containing the polymer was washed with a saturated aqueous $NaHCO_3$ solution (4 mL) and water (4 mL) and then subjected to the GPC measurement to determine the molecular weight and its distribution of the treated polymer.

Blend Film Preparation. A neat blend film composed of fPOSS−PMMA and PMMA was prepared by spin-coating a mixture of the two polymers dissolved in dioxane, which had been passed through a Teflon filter (Cosmonice Filter S, pore size = 0.45 μm, Nihon Millipore Ltd., Tokyo, Japan) beforehand, onto a clean silicon wafer at 2500 rpm for 50 s. The concentration of the polymer solution was 4 wt %. The spin-coated film was dried in a temperature-controlled vacuum oven at 25 °C for 12 h. The dried film was annealed under vacuum at 180 °C for 5 days and then cooled to room temperature under vacuum.

Ar^+ Ion Etching. A blend film was etched with an Ar^+ ion beam operated at 2 kV of acceleration voltage for 1.2 min. The system pressure was 7.5×10^{-7} Torr. The etched depth of the film was measured by an Alpha-Step 200 surface profiler system (Tencor Instruments Co., Ltd.).

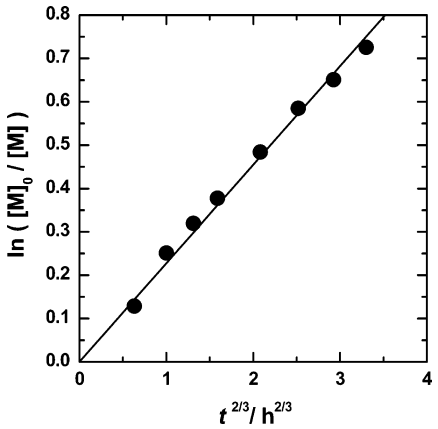

Figure 1. Plot of $\ln([M]_0/[M])$ vs $t^{2/3}$ for the solution polymerization of MMA (50 wt %) in DMF at 70 °C with 7F-T_8-BIB: $[MMA]_0/[7F\text{-}T_8\text{-}BIB]_0/[Cu(I)Cl]_0/[dNbipy]_0 = 400/1/1/2$.

Results and Discussion

Synthesis of the Fluorinated POSS-Holding Initiator 7F-T_8-BIB. The fluorinated POSS derivative with an initiating site for ATRP was synthesized by the method described above: in short, (3,3,3-trifluoropropyl)trimethoxysilane was hydrolytically condensed in the presence of sodium hydroxide to obtain incompletely condensed, fluorinated POSS with the highly reactive group of trisodium silanolate, 7F-T_7-$(ONa)_3$, which was subsequently corner-capped with acetoxyethyltrichlorosilane to give 7F-T_8-AE. The acetoxy group of 7F-T_8-AE was deprotected by the acid treatment to obtain hydroxyl group-carrying POSS (7F-T_8-HE). Finally, the acylation of 7F-T_8-HE with 2-bromoisobutyryl bromide gave the fluorinated POSS-holding initiator 7F-T_8-BIB in a moderate overall yield of 40%. Its high purity was confirmed by ^{1}H, ^{13}C, and ^{29}Si NMR and elemental analysis. The solubility of 7F-T_8-BIB in various organic solvents (1 wt %) was checked by the naked eye observation. 7F-T_8-BIB is soluble in DMF, dimethyl sulfoxide, *N*,*N*′-dimethylacetamide, and MMA, partly soluble in anisole, toluene, acetone, and THF, and insoluble in hexane and diphenyl ether.

ATRP of MMA Initiated by 7F-T_8-BIB. 7F-T_8-BIB was employed for solution polymerization of MMA with a copper complex in DMF at 70 °C. DMF was chosen as a solvent for the solubility of 7F-T_8-BIB. Soon after the reaction mixture was heated at 70 °C, no trace of Cu(I)Cl powder was observed in the system. The color of the homogeneous solution was originally dark brown and turned to reddish brown as the polymerization proceeded. In an ATRP with no conventional initiation and no Cu(II) concentration at the onset of polymerization ($t = 0$), the polymerization rate should show the 2/3-order time dependence of conversion index $\ln([M]_0/[M])$.[31,32] Thus, we made the plot of $\ln([M]_0/[M])$ vs $t^{2/3}$ for our polymerization system, as shown in Figure 1. The plot can be approximated by a straight line passing through the origin. This means that the polymerization kinetics of this system can be well understood in terms of the power-law theory, at least under the studied experimental conditions.

Figure 2a shows the GPC traces of the obtained polymers. With increasing reaction time, the mass distribution shifts to a higher molar mass region, becoming broader and eventually bimodal at $t = 6$ h. This may be due to the fluorinated POSS moiety at the end of the polymer chain, which may cause aggregation

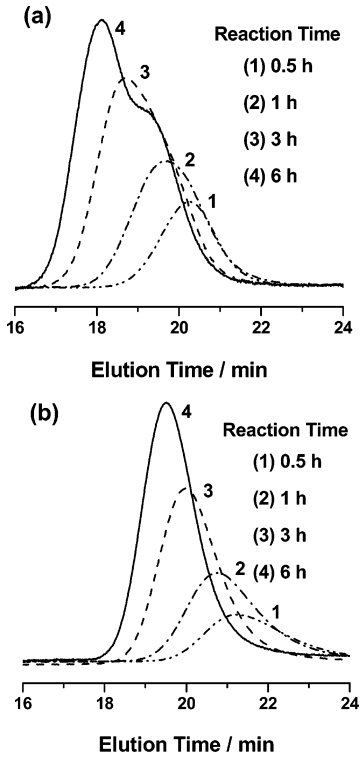

Figure 2. GPC traces of fPOSS−PMMAs (a) before and (b) after the HF treatment.

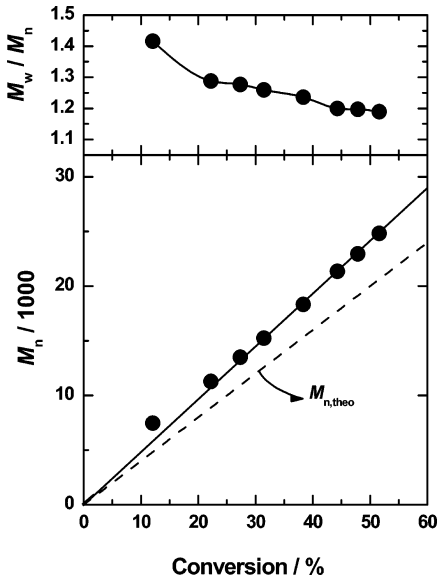

Figure 3. Evolution of M_n and M_w/M_n of HF-treated fPOSS−PMMAs as a function of monomer conversion. The broken line in the figure represents the theoretical prediction.

of the polymer. To avoid this, the POSS moiety was decomposed by the HF treatment. The mass distribution became narrower, and the shoulder peak observed before the HF treatment completely disappeared (Figure 2b). Figure 3 shows the evolution of the number-average molecular weight M_n and the polydispersity index M_w/M_n of the HF-treated polymer. It can be seen that the M_n increases linearly with increasing monomer conversion. These M_n values, however, are slightly larger than the theoretical values $M_{n,theo}$ calculated with the initial molar ratio of MMA and the initiator 7F-T_8-BIB, for a still unclear reason. To check the validity of the GPC analysis after the HF treatment, we carried out ^{1}H NMR

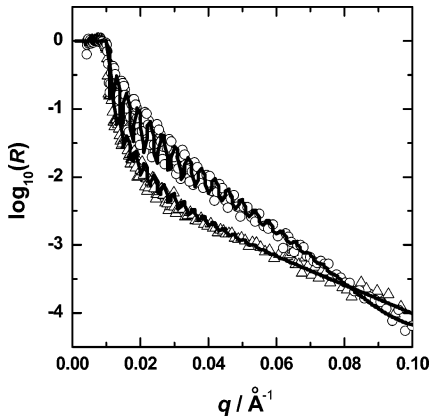

Figure 4. Neutron reflectivity profiles obtained for the fPOSS−dPMMA/PMMA blend films composed of 20 wt % of fPOSS−dPMMA (M_n = 12 000 and M_w/M_n = 1.13) and 80 wt % of PMMA (M_n = 180 000 and M_w/M_n = 1.09) before (△) and after (○) annealing the films at 180 °C for 5 days. The full lines in the figure represent the best fit for the data on the basis of the multilayered model using the spreadsheet environment reflectivity fitting.

measurement for one sample before the HF treatment and estimated the M_n of the PMMA segment to be 7300 on the basis of the numbers of the methylene protons of the polymer backbone and the ester protons of the POSS moiety. This value is in good agreement with the GPC value of 7500 (after the HF treatment). The M_w/M_n ratio decreases with increasing monomer conversion, reaching 1.2 at conversion about 45% or larger. All these results confirm that the ATRP of MMA with 7F-T_8-BIB proceeds in a living fashion, providing a low-polydispersity, tadpole-shaped hybrid polymer with an "inorganic head" of fluorinated POSS and an "organic tail" of PMMA (fPOSS−PMMA).

Surface Characterizations of POSS-Containing Thin Films. Fluorinated substances in a polymer film tend to get concentrated (enriched) at the air/polymer interface.[21−25] We carried out the surface characterization of a ultrathin blend film composed of a fPOSS−PMMA (M_n = 12 000) and a PMMA (M_n = 180 000). This film, denoted fPOSS−PMMA/PMMA, was prepared by spin-casting a solution of the two polymers in dioxane on a silicon wafer and had a thickness of several hundred nanometers.

Neutron reflectivity measurements were undertaken to examine the overall structure of the fPOSS−dPMMA/PMMA blend film. The use of a deuterated polymer affords a high contrast in scattering length density between the deuterated and hydrogenous components. The deuterated fPOSS−PMMA (fPOSS−dPMMA) with M_n = 12 000 and M_w/M_n = 1.13 was similarly prepared by ATRP of deuterated MMA initiated with 7F-T_8-BIB. Figure 4 shows the neutron reflectivity R as a function of the wave vector q for the blend film composed of 20 wt % of fPOSS−dPMMA and 80 wt % of PMMA (M_n = 180 000, M_w/M_n = 1.09), measured before and after annealing the film at 180 °C for 5 days. The regular interference fringes that tend to dampen in height at high q suggest the existence of a layered structure. Attempts to model the neutron reflectivity profiles with two- or three-layered structures were carried out. Satisfactory fitting was obtained only by assuming the three-layered structure with two fPOSS−dPMMA-enriched layers at the air/polymer and polymer/silicon interfaces and a bulk layer flanked by them (Figure 4).

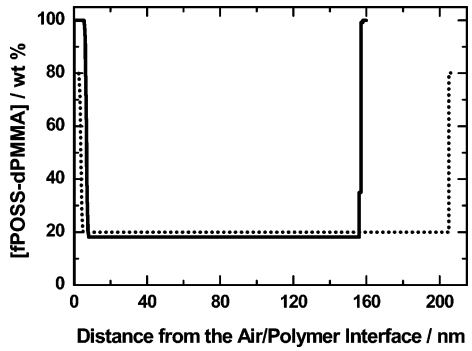

Figure 5. Weight fraction profiles of fPOSS−dPMMA as a function of the distance from the air/polymer interface for the fPOSS−dPMMA/PMMA blend films composed of 20 wt % of fPOSS−dPMMA (M_n = 12 000 and M_w/M_n = 1.13) and 80 wt % of PMMA (M_n = 180 000 and M_w/M_n = 1.09) before (dotted line) and after (full line) annealing the films at 180 °C for 5 days.

The gradient region between the fPOSS−dPMMA-enriched and bulk layers was calculated by matching the scattering length densities of the two adjacent layers on the basis of the error function.[30] The weight fraction of fPOSS−dPMMA was calculated from the scattering length density profiles obtained by the parameters for the best fittings in Figure 4. Figure 5 shows the weight fraction profiles of fPOSS−dPMMA as a function of the distance from the air/polymer interface. fPOSS−dPMMA is more populated at the air/polymer and polymer/silicon interfaces, and this behavior is more pronounced for the annealed film. For the annealed film, the weight fraction of the deuterated component reaches about 100% at the two interfaces. The thinning of the annealed film, which is apparent in Figure 5, was caused by the removal of solvents and air by annealing.

To verify that the enrichment of fPOSS−dPMMA is ascribed to the inherent property of the fluorinated material, we carried out similar experiments using two different polymers instead of fPOSS−dPMMA. One, PhPOSS−dPMMA, was synthesized by ATRP of deuterated MMA initiated with 2-bromoisobutyryloxyethylheptaphenyl-T_8-silsesquioxane,[27] and the other, EIB-dPMMA, was synthesized by ATRP of deuterated MMA initiated with ethyl 2-bromoisobutylate. PhPOSS−dPMMA (M_n = 9000, M_w/M_n = 1.08) had the POSS end group substituted with phenyl groups, and EIB−dPMMA (M_n = 13 000, M_w/M_n = 1.14) had an ethyl isobutyrate end group. Figure 6 shows the weight fraction profiles of the deuterated components in the PhPOSS−dPMMA/PMMA and EIB−dPMMA/PMMA blend films annealed at 180 °C for 5 days. The PMMA matrix sample (M_n = 180 000, M_w/M_n = 1.09) was the same in all experiments. The figure shows that PhPOSS−dPMMA is again enriched at the two interfaces, but the extent of enrichment is much lower (about 50% of weight fraction of the deuterated component) than in the case of fPOSS−dPMMA. Interestingly, a minor surface enrichment of the deuterated species was also observed for the EIB−dPMMA/PMMA film. This is ascribed to the difference in molecular weight[33] or that in end group or both. The energy difference between deuterium and hydrogen should be less important in this problem. These results confirm that the major driving force for the remarkable surface enrichment of fPOSS−dPMMA observed for the annealed fPOSS−dPMMA/PMMA blend film is the low surface free energy of the fluorinated POSS. The POSS polymer itself has

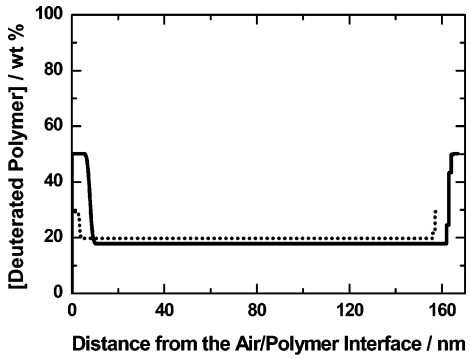

Figure 6. Weight fraction profiles of deuterated PMMA (PhPOSS−dPMMA or EIB−dPMMA) as a function of the distance from the air/polymer interface for the PhPOSS−dPMMA/PMMA (full line) blend film composed of 20 wt % of PhPOSS−dPMMA (M_n = 9000 and M_w/M_n = 1.08) and 80 wt % of PMMA (M_n = 180 000 and M_w/M_n = 1.09) and the EIB−dPMMA/PMMA (dotted line) blend film composed of 20 wt % of EIB−dPMMA (M_n = 13 000 and M_w/M_n = 1.14) and 80 wt % of PMMA (M_n = 180 000 and M_w/M_n = 1.09) after annealing the films at 180 °C for 5 days.

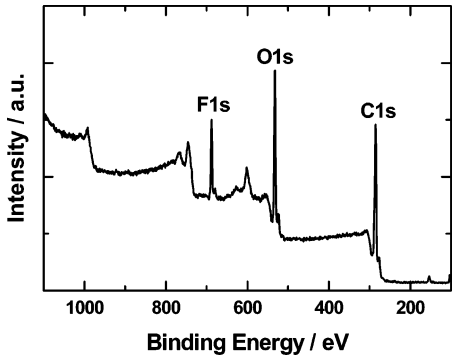

Figure 7. XPS survey spectrum of the fPOSS−PMMA/PMMA blend film composed of 20 wt % of fPOSS−PMMA (M_n = 12 000 and M_w/M_n = 1.18) and 80 wt % of PMMA (M_n = 180 000 and M_w/M_n = 1.09) after annealing the film at 180 °C for 5 days. The measurement was carried out at 90° takeoff angle.

a significant tendency to segregating at the surfaces, which is highly strengthened by fluorination.

The neutron reflectometry for the fPOSS−dPMMA/PMMA blend film revealed that fPOSS−dPMMA gets populated at the air/polymer interface, forming the top layer composed of nearly pure fPOSS−dPMMA of thickness about 10 nm. A question now arises as to the distribution of fluorinated POSS moieties attached to the polymer chain end within the top layer. To clarify this, we made an angle-dependent XPS measurement, which allows us to determine the surface composition as a function of depth. The takeoff angles used here were 15°, 30°, 45°, 60°, 75°, and 90°, which approximately corresponded to the total sampling depth of 2.1, 4.1, 5.8, 7.1, 7.9, and 8.2 nm, respectively.[34] Figure 7 shows the XPS survey spectrum taken at takeoff angle 90° for an annealed blend film of thickness 220 nm composed of 20 wt % of fPOSS−PMMA (M_n = 12 000 and M_w/M_n = 1.18) and 80 wt % of PMMA (M_n = 180 000 and M_w/M_n = 1.09). Clearly observed are a F 1s peak at 687.9 eV attributable to the fluoroalkyl chain of the POSS moiety and O 1s and C 1s peaks at 531.9 and 284.7 eV, respectively, attributable to both the POSS moiety and the PMMA chain. Qualitatively similar spectra were obtained at different takeoff angles. The depth profile of the atomic molar ratio of fluorine and carbon was estimated by determining the areas of the F 1s and C

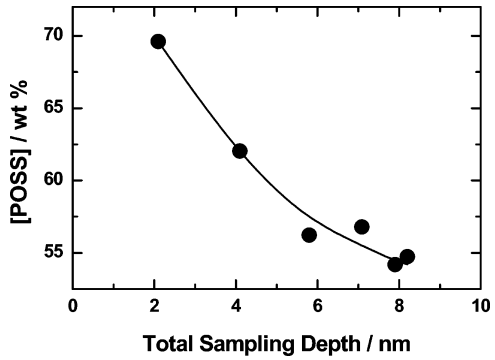

Figure 8. Weight fraction profile of POSS as a function of the total sampling depth in the XPS measurements carried out at the different takeoff angles for the fPOSS−PMMA/PMMA blend film composed of 20 wt % of fPOSS−PMMA (M_n = 12 000 and M_w/M_n = 1.18) and 80 wt % of PMMA (M_n = 180 000 and M_w/M_n = 1.09) after annealing the film at 180 °C for 5 days.

1s peaks and multiplying them by appropriate sensitivity factors, with which the weight fraction of POSS was calculated using the known molar mass and atomic molar ratio of the POSS moiety and MMA unit. Figure 8 shows the POSS weight fraction profile as a function of the total sampling depth. The weight fraction of POSS increases with decreasing total sampling depth, exceeding 70 wt % for total sampling depth smaller than 2 nm. This means that the POSS moieties are highly and the most populated at the outermost surface of the film.

The same fPOSS−PMMA/PMMA blend film was subjected to contact angle measurements with water and diiodomethane as probe liquids. The contact angles of water (θ_w) and diiodomethane (θ_{dim}) were estimated to be 83.7° and 55.9°, respectively (cf. θ_w and θ_{dim} with PMMA film were 66.5° and 33.6°, respectively). Using the well-known geometric mean model[35] and the measured contact angles, we calculated the surface free energy of the blend film to be 33.1 mN/m. This value is close to the surface free energy (32.5 mN/m) of a glass slide treated with the silane coupling agent (3,3,3-trifluoropropyl)trimethoxysilane. This result suggests that the outermost layer of the blend film is almost completely covered by the POSS moieties.

Etching Resistance of the fPOSS−PMMA/PMMA Blend Film. Gonsalves et al.[36] and Argitis et al.[37] reported that the incorporation of POSS in methacrylate-based resists by copolymerizations of methacrylates with POSS-carrying monomers significantly improved resistance against reactive ion etching in O_2 plasma, if the POSS content in the resists exceeded 20−30 wt %. We have examined effects of surface enrichment of the POSS units on the etching behavior of the fPOSS−PMMA/PMMA blend film.

A fPOSS−PMMA/PMMA blend film similar to those used for the XPS and contact angle measurements was used for the etching study. For reference, a blend film containing 20 wt % of a relatively short PMMA (M_n = 13 000) and 80 wt % of a relatively long one (M_n = 180 000) was also studied. Both films were annealed at 180 °C for 5 days and then subjected to Ar^+ ion etching for 1.2 min. As shown in Table 1, the etched depth measured for the reference sample (without POSS moieties) is about 5 times larger than that for the fPOSS−PMMA/PMMA blend film. This shows strong resistance of the POSS-containing blend film against the Ar^+ ion etching.

Table 1. Results of Ar^+ Ion Etching for Blend Films[a]

sample	etched depth (nm)
fPOSS−PMMA/PMMA[b]	20
PMMA/PMMA[c]	95

[a] The Ar^+ ion etching was carried out at 2 kV of acceleration voltage for 1.2 min. [b] Blend film with POSS composed of 20 wt % of fPOSS−PMMA (M_n = 12 000) and 80 wt % of PMMA (M_n = 180 000). [c] Blend film without POSS composed of 20 wt % of PMMA (M_n = 12 000) and 80 wt % of PMMA (M_n = 180 000).

Gonsalves et al.[36] explained their result of the improved etching resistance of the POSS-containing copolymer by the following two reasons: First, inorganic molecules such as POSS generally have high etching resistance than organic molecules. Second, the POSS units in the polymer assume a different morphology, forming large rectangular crystallites, when the POSS content exceeds a certain level, say, 20−30 wt %.[10,38,39] A network of these rectangular crystallites uniformly distributed within the polymer matrix will effectively protect the polymers from the O_2 plasma etching. In our fPOSS−PMMA/PMMA blend film, some kind of crystallites of the POSS moieties can be formed on the top surface of the film highly enriched with the POSS moieties, which will afford the strong resistance against the Ar^+ ion etching. The most important and interesting point in our system is that the overall POSS content in the blend film is only 2 wt %, as is calculated from the weight fraction of fPOSS−PMMA in the blend film (20 wt %) and that of the POSS moiety in the fPOSS−PMMA chain (10 wt %). This POSS content (2 wt %) is an order of magnitude smaller than the critical content (20−30 wt %), above which the important effects of POSS were noted in the previous reports.[36,37] Thus, the surface enrichment of the POSS moieties strongly effected by the fluorination was confirmed to provide the film with a remarkably enhanced etching resistance.

Conclusions

A new POSS-holding initiator for ATRP was designed and used to synthesize a tadpole-shaped hybrid polymer with an "inorganic head" of fluorinated POSS and an "organic tail" of well-defined PMMA. Neutron reflectometric, XPS, and contact angle measurements for an annealed blend film composed of the hybrid polymer and PMMA showed that the POSS moieties in the film were highly populated on the ourtermost surface of the film. Because of this unique structure, the blend film exhibited strong resistance against Ar^+ ion etching.

Supporting Information Available: Synthetic method and ^1H, ^{13}C, and ^{29}Si NMR data of 7F-T_7-$(OTMS)_3$. This material is available free of charge via the Internet at http://pubs.acs.org.

References and Notes

(1) (a) Provatas, A.; Matisons, J. G. *Trends Polym. Sci.* **1997**, *5*, 327−332. (b) Baney, R. H.; Itoh, M.; Sakakibara, A.; Suzuki, T. *Chem. Rev.* **1995**, *95*, 1409−1430. (c) Pescarmona, P. P.; Maschmeyer, T. *Aust. J. Chem.* **2001**, *54*, 583−596. (d) Laine, R. M.; Zhang, C.; Sellinger, A.; Viculis, L. *Appl. Organomet. Chem.* **1998**, *12*, 715−723.

(2) (a) Pittman, C. U., Jr.; Li, G. Z.; Ni, H. *Macromol. Symp.* **2003**, *196*, 301−325. (b) Li, G. Z.; Wang, L.; Ni, H.; Pittman, C. U., Jr. *J. Inorg. Organomet. Polym.* **2001**, *11*, 123−154.

(3) (a) Schwab, J. J.; Lichtenhan, J. D. *Appl. Organomet. Chem.* **1998**, *12*, 707−713. (b) Lichtenhan, J. D.; Otonari, Y. A.; Carr,

M. J. *Macromolecules* **1995**, *28*, 8435−8437. (c) Haddad, T. S.; Lichtenhan, J. D. *Macromolecues* **1996**, *29*, 7302−7304.
(4) (a) Xu, H.; Kuo, S. W.; Lee, J. S.; Chang, F. C. *Macromolecules* **2002**, *35*, 8788−8793. (b) Zhang, W.; Fu, B. X.; Seo, Y.; Schrag, E.; Hsiao, B.; Mather, P.; Yang, N. L.; Xu, D.; Ade, H.; Rafailovich, M.; Sokolov, J. *Macromolecules* **2002**, *35*, 8029−8038.
(5) (a) Neumann, D.; Fisher, M.; Tran, L.; Matisons, J. G. *J. Am. Chem. Soc.* **2002**, *124*, 13998−13999. (b) Choi, J.; Kim, S. G.; Laine, R. M. *Macromolecules* **2004**, *37*, 99−109. (c) Sellinger, A.; Laine, R. M. *Macromolecules* **1996**, *29*, 2327−2330. (d) Choi, J.; Harcup, J.; Yee, A. F.; Zhu, Q.; Laine, R. M. *J. Am. Chem. Soc.* **2001**, *123*, 11420−11430.
(6) Maitra, P.; Wunder, S. L. *Chem. Mater.* **2002**, *14*, 4494−4497.
(7) Kim, K.-M.; Keum, D.-K.; Chujo, Y. *Macromolecules* **2003**, *36*, 867−875.
(8) (a) Pyun, J.; Xia, J.; Matyjaszewski, K. *ACS Symp. Ser.* **2003**, *838*, 273−284. (b) Pyun, J.; Matyjaszewski, K.; Wu, J.; Kim, G.-M.; Chun, S. B.; Mather, P. T. *Polymer* **2003**, *44*, 2739−2750. (c) Matyjaszewski, K.; Miller, P. J.; Kickelbick, G.; Nakagawa, Y.; Diamanti, S.; Pacis, C. *ACS Symp. Ser.* **2000**, *729*, 270−283.
(9) Costa, R. O. R.; Vasconcelos, W. L.; Tamaki, R.; Laine, R. M. *Macromolecules* **2001**, *34*, 5398−5407.
(10) Fu, B. X.; Lee, A.; Haddad, T. S. *Macromolecules* **2004**, *37*, 5211−5218.
(11) Lee, Y. J.; Kuo, S. W.; Huang, W. J.; Lee, H. T.; Chang, F. C. *J. Polym. Sci., Part B: Polym. Phys.* **2004**, *42*, 1127−1136.
(12) Matejka, L.; Dukh, O.; Meissner, B.; Hlavata, D.; Brus, J.; Strachota, A. *Macromolecules* **2003**, *36*, 7977−7985.
(13) Li, G. Z.; Wang, L. C.; Toghiani, H.; Daulton, T. L.; Koyama, K.; Pittman, C. U., Jr. *Macromolecules* **2001**, *34*, 8686−8693.
(14) Zheng, L.; Farris, R. J.; Coughlin, E. B. *Macromolecules* **2001**, *34*, 8034−8039.
(15) Phillips, S. H.; Haddad, T. S.; Tomczak, S. J. *Curr. Opin. Solid State Mater. Sci.* **2004**, *8*, 21−29.
(16) Isayeva, I. S.; Kennedy, J. P. *J. Polym. Sci., Part A: Polym. Chem.* **2004**, *42*, 4337−4352.
(17) (a) Romo-Uribe, A.; Mather, P. T.; Haddad, T. S.; Lichtenhan, J. D. *J. Polym. Sci., Part B: Polym Phys.* **1998**, *36*, 1857−1872. (b) Mather, P. T.; Jeon, H. G.; Romo-Uribe, A.; Haddad, T. S.; Lichtenhan, J. D. *Macromolecules* **1999**, *32*, 1194−1203.
(18) Li, G. Z.; Wang, H.; Toghiani, T. L.; Daulton, T. L.; Pittman, C. U., Jr. *Polymer* **2002**, *43*, 4167−4176.
(19) Koberstein, J. T. *J. Polym. Sci., Part B: Polym. Phys.* **2004**, *42*, 2942−2956.
(20) Feast, W. J., Munro, H. S., Richarsa, R. W., Eds.; *Polymer Surface and Interfaces II*; John Wiley & Sons: Chichester, 1993.
(21) Li, X. F.; Chiellini, E.; Galli, G.; Ober, C. K.; Hexemer, A.; Kramer, E. J.; Fischer, D. A. *Macromolecules* **2002**, *35*, 8078−8087.
(22) Youngblood, J. P.; McCarthy, T. J. *Macromolecules* **1999**, *32*, 6800−6806.
(23) O'Rourke-Muisener, P. A. V.; Jalbert, C. A.; Yuan, C.; Baetzold, J.; Mason, R.; Wong, D.; Kim, Y. J.; Koberstein, J. T.; Gunesin, B. *Macromolecules* **2003**, *36*, 2956−2966.
(24) Affrossman, S.; Bertrand, P.; Hartshorne, M.; Kiff, T.; Leonard, D.; Pethrick, R. A.; Richards, R. W. *Macromolecules* **1996**, *29*, 5432−5437.
(25) Hirao, A.; Koide, G.; Sugiyama, K. *Macromolecules* **2002**, *35*, 7642−7651.
(26) Oikawa, H.; Yoshida, K.; Iwatani, K.; Watanabe, K.; Ootake, N. International Pat. Appl. PCT/JP02/94776 WO02/094839 (17 May, 2002); *Chem. Abstr.* **2002**, *138*, 5844. (b) Morimoto, Y.; Ito, K.; Oikawa, H.; Yamahiro, M.; Watanabe, K.; Ootake, N. U.S. Pat. Appl. US 2004030084 (12 February, 2004); *Chem. Abstr.* **2004**, *140*, 164688.
(27) Ohno, K.; Sugiyama, S.; Koh, K.; Tsujii, Y.; Fukuda, T.; Yamahiro, M.; Oikawa, H.; Yamamoto, Y.; Ootake, N.; Watanabe, K. *Macromolecules* **2004**, *37*, 8517−8522.
(28) (a) Patten, T. E.; Xia, J.; Abernathy, T.; Matyjaszewski, K. *Science* **1996**, *272*, 866−868. (b) Matyjaszewski, K.; Xia, J. In *Handbook of Radical Polymerization*; Matyjaszewski, K., Davis, T. P., Eds.; John Wiley & Sons: Hoboken, NJ, 2002; pp 523−628.
(29) Takeda, M.; Endoh, Y. *Physica B* **1999**, *267−268*, 185−189.
(30) Welp, K. A.; Co, C. C.; Wool, R. P. *J. Neutron Res.* **1999**, *185*, 267−268.
(31) (a) Fischer, H. *Macromolecules* **1997**, *30*, 5666−5672. (b) Fisher, H. *J. Polym. Sci., Part A: Polym. Chem.* **1999**, *37*, 1985−1901. (c) Fischer, H. *Chem. Rev.* **2001**, *101*, 3581−3610.
(32) (a) Ohno, K.; Tsujii, Y.; Miyamoto, T.; Fukuda, T.; Goto, M.; Kobayashi, K.; Akaike, T. *Macromolecules* **1998**, *31*, 1064−1069. (b) Yoshikawa, C.; Goto, A.; Fukuda, T. *Macromolecules* **2003**, *36*, 908−912. (c) Goto, A.; Fukuda, T. *Prog. Polym. Sci.* **2004**, *29*, 329−385. (d) Fukuda, T. *J. Polym. Sci., Part A: Polym. Chem.* **2004**, *42*, 4743−4755.
(33) (a) Tanaka, K.; Kajiyama, T.; Takahara, A.; Tasaki, S. *Macromolecules* **2002**, *35*, 4702−4706. (b) Bitsanis, I. A.; ten Brinke, G. *J. Chem. Phys.* **1993**, *99*, 3100−3111. (c) Hariharan, A.; Kumar, S. K.; Russell, T. P. *J. Chem. Phys.* **1993**, *99*, 4041−4050.
(34) (a) Jablonski, A.; Powell, C. J. *Surf. Sci. Rep.* **2002**, *47*, 33−91. (b) Roberts, R. F.; Allara, D. L.; Pryde, C. A.; Buchanan, D. N. E.; Hobbins, N. D. *Surf. Interface Anal.* **1980**, *2*, 5−10. (c) Seah, M. P.; Dench, W. A. *Surf. Interface Anal.* **1979**, *1*, 2−11.
(35) (a) Kaelble, D. H.; Uy, K. C. *J. Adhes.* **1970**, *2*, 50−60. (b) Owens, D. K.; Wendt, R. C. *J. Appl. Polym. Sci.* **1969**, *13*, 1741−1747.
(36) Wu, H.; Hu, Y.; Gonsalves, K. E.; Yacaman, M. J. *J. Vac. Sci. Technol. B* **2001**, *19*, 851−855.
(37) (a) Bellas, V.; Tegou, E.; Raptis, I.; Gogolides, E.; Argitis, P.; Iatrou, H.; Hadjichristidis, N.; Sarantopoulou, E.; Cefalas, A. C. *J. Vac. Sci. Technol. B* **2002**, *20*, 2902−2908. (b) Tegou, E.; Bellas, V.; Gogolides, E.; Argitis, P.; Eon, D.; Cartry, G.; Cardinaud, C. *Chem. Mater.* **2004**, *16*, 2567−2577.
(38) Leu, C.-M.; Chang, Y.-T.; Wei, K.-H. *Macromolecules* **2003**, *36*, 9122−9127.
(39) Zheng, L.; Hong, S.; Cardoen, G.; Burgaz, E.; Gido, S. P.; Coughlin, E. B. *Macromolecules* **2004**, *37*, 8606−8611.

MA047636L